

Article

Galaxy Formation, Evolution and Rotation as a 4D Relativistic Cloud-World Embedded in a 4D Conformal Bulk: From String to Cloud Theory

Mohammed B. Al-Fadhli^{1,*}

¹ College of Science, University of Lincoln, Lincoln, LN6 7TS, UK.

* Correspondence: malfadhli@lincoln.ac.uk; mo.fadhli7@gmail.com

Abstract: The recent observation of the G2 gas cloud orbit around the galactic centre has challenged the model of a mere supermassive black hole that should have destroyed it. In addition, the Planck Legacy 2018 (PL18) release has preferred a positively curved early Universe with a confidence level exceeding 99%. In this study, the formation of a galaxy from the collapse of a supermassive gas cloud in the early Universe is modelled based on extended field equations as a 4D relativistic cloud-world that flows and spins through a 4D conformal bulk of an initial positive curvature considering the preference of the PL18 release. Owing to the curved background, this scenario of galaxy formation reveals that the core of the galaxy undergoes a forced vortex formation with a central event horizon leading to opposite vortices (traversable wormholes) that are spatially shrinking through evolving in the conformal time. It indicates that the galaxy and its core are formed at the same process where the surrounding gas clouds form the spiral arms due to the frame-dragging induced by the fast-rotating core. Further, the bulk conformal curvature evolution demonstrates the fast orbital speed of outer stars owing to external fields exerted on galaxies as they travel through conformally curved space-time. Accordingly, the G2 gas cloud that only faced the drag effects could be explained if its orbit is around the vortex but at a distance from the central event horizon. These findings could explain the fast orbital speed of outer stars where the galaxy formation and its core simultaneously could explain the formation of the supermassive compact galaxy cores with a mass of $\sim 10^9 M_{\odot}$ at just 6% of the current Universe age and thus could resolve the black hole hierarchy problem.

Keywords: Galaxy Formation; Conformal Spacetime; Brane-World Modified Gravity.

1. Introduction

Observations from the Deep Extragalactic Evolutionary Probe 2 Survey of a large sample of disk galaxies found that the motions of galaxies were steadily getting in order with the rotation velocity increasing over the last eight billion years [1,2]. In addition, the galactic rotation curves were found to be influenced by external fields [3] and follow the baryonic Tully-Fisher relation [4,5]. Further, the Dark Energy Survey Collaboration has recently released the largest maps of galaxy distribution and shapes, which showed that dark matter is more distributed than that predicted by General Relativity [6,7]. On the other hand, some studies reported that some galaxies are missing dark matter [8–10].

To get insights from these observations while aiming to explain the G2 cloud's observation that has challenged the model of a mere supermassive black hole at the centre of our galaxy [11,12], this study presents a new galaxy formation scenario considering the background curvature as preferred by the Planck Legacy 2018 (PL18) release; where the PL18 release has confirmed the presence of an enhanced lensing amplitude in the cosmic microwave background power spectra, which prefers a positively curved early Universe with a confidence level greater than 99% [13,14]. In addition, the induced spacetime curvature by the entire galaxy differs from one galaxy to another due to their diverse energy densities, thus, celestial objects in different galaxies experience different background or bulk curvatures.

2. Interaction Field Equations

The PL18 release has preferred a positively curved early Universe, that is, is a sign of a global background curvature or a curved bulk. To incorporate the bulk curvature and its evolution over the conformal time, a modulus of the spacetime deformation, E_D , is introduced based on the theory of elasticity [15]. E_D = (stress/strain) is in terms of energy density and it can be expressed by using Einstein field equations or in the Lagrangian formulation of the electromagnetic potential energy density in space representing the energy density existing in the bulk that is considered as the global inertial frame of reference for the embedded celestial objects as follows

$$E_D = \frac{T_{\mu\nu} - T g_{\mu\nu}/2}{R_{\mu\nu}/\mathcal{R}} = \int_B -\frac{F_{\alpha\lambda}F^{\alpha\lambda}}{4\mu_0} d^4\sigma \quad (1)$$

where the stress is signified by the stress-energy tensor $T_{\mu\nu}$ of trace T while the strain is signified by the Ricci curvature tensor $R_{\mu\nu}$ as the change in the curvature divided by the scalar of the bulk curvature \mathcal{R} while $F_{\alpha\beta}$ is the field strength tensor using a metric of signature $(-,+,+,+)$ and μ_0 is vacuum permeability. By incorporating the bulk influence, the Einstein–Hilbert action can be extended to

$$S = E_D \int_C \left[\frac{R}{\mathcal{R}} + \frac{L}{\mathcal{L}} \right] \sqrt{-g} d^4\rho \quad (2)$$

where R is the Ricci scalar curvature representing a localized curvature induced by a celestial object that is regarded as a 4D relativistic cloud-world of a metric tensor $g_{\mu\nu}$ and Lagrangian density L on local relativistic coordinate system ρ . \mathcal{R} represents the scalar curvature of the 4D bulk of metric tensor $\tilde{g}_{\mu\nu}$ on global conformal coordinate system σ while \mathcal{L} is the bulk's Lagrangian density as a manifestation of its internal stresses and momenta reflecting its curvature. The evolution of the bulk curvature over the conformal time can be characterized by Weyl's conformal transformation as $\tilde{g}_{\mu\nu} = g_{\mu\nu}\Omega^2$ where Ω^2 is a conformal function [16]. To consider the bulk expansion over the conformal time (the expansion of the Universe), a dual-action concerning the conservation of energy on global (bulk) and local (cloud-world) scales is introduced as follows

$$S = \int_B \left[-\frac{F_{\alpha\lambda}\tilde{g}^{\alpha\gamma}F_{\gamma\rho}\tilde{g}^{\lambda\rho}}{8\mu_0} \right] \sqrt{-\tilde{g}} \int_C \left[\frac{R_{\mu\nu}g^{\mu\nu}}{\mathcal{R}_{\mu\nu}\tilde{g}^{\mu\nu}} + \frac{L_{\mu\nu}g^{\mu\nu}}{\mathcal{L}_{\mu\nu}\tilde{g}^{\mu\nu}} \right] \sqrt{-g} d^4\rho d^4\sigma \quad (3)$$

The global-local action should hold for any variation as

$$\delta S = \int_B \left[\frac{-\delta(\tilde{g}^{\alpha\gamma}\tilde{g}^{\lambda\rho})F_{\alpha\lambda}F_{\gamma\rho}\sqrt{-\tilde{g}}}{8\mu_0} \right] \int_C \left[\frac{\delta(R_{\mu\nu}g^{\mu\nu})\sqrt{-g}}{\mathcal{R}_{\mu\nu}\tilde{g}^{\mu\nu}} - \frac{\delta(\mathcal{R}_{\mu\nu}\tilde{g}^{\mu\nu})R_{\mu\nu}g^{\mu\nu}\sqrt{-g}}{(\mathcal{R}_{\mu\nu}\tilde{g}^{\mu\nu})^2} + \frac{R_{\mu\nu}g^{\mu\nu}\delta\sqrt{-g}}{\mathcal{R}_{\mu\nu}\tilde{g}^{\mu\nu}} \right. \\ \left. + \frac{\delta(L_{\mu\nu}g^{\mu\nu})\sqrt{-g}}{\mathcal{L}_{\mu\nu}\tilde{g}^{\mu\nu}} - \frac{\delta(\mathcal{L}_{\mu\nu}\tilde{g}^{\mu\nu})L_{\mu\nu}g^{\mu\nu}\sqrt{-g}}{(\mathcal{L}_{\mu\nu}\tilde{g}^{\mu\nu})^2} + \frac{L_{\mu\nu}g^{\mu\nu}\delta\sqrt{-g}}{\mathcal{L}_{\mu\nu}\tilde{g}^{\mu\nu}} \right] d^4\rho d^4\sigma \quad (4)$$

By utilizing Jacobi's formula, $\delta\sqrt{-g} = -\sqrt{-g} g_{\mu\nu}\delta g^{\mu\nu}/2$ [18]. Hence, the variation is

$$\delta S = \int_B \left[\frac{-\frac{F_{\alpha\lambda}\delta\tilde{g}^{\alpha\gamma}F_{\gamma\rho}\tilde{g}^{\lambda\rho}}{4\mu_0} + \frac{F_{\alpha\lambda}\tilde{g}^{\alpha\gamma}F_{\gamma\rho}\tilde{g}^{\lambda\rho}\tilde{g}_{\mu\nu}\delta\tilde{g}^{\mu\nu}}{16\mu_0}} \right] \sqrt{-\tilde{g}} \int_C \left[\frac{R_{\mu\nu}\delta g^{\mu\nu} + g^{\mu\nu}\delta R_{\mu\nu}}{\mathcal{R}} - \frac{R_{\mu\nu}\delta\tilde{g}^{\mu\nu} + \tilde{g}^{\mu\nu}\delta\mathcal{R}_{\mu\nu}}{\mathcal{R}^2} R - \frac{g_{\mu\nu}\delta g^{\mu\nu}}{2\mathcal{R}} R \right. \\ \left. + \frac{L_{\mu\nu}\delta g^{\mu\nu} + g^{\mu\nu}\delta L_{\mu\nu}}{\mathcal{L}} - \frac{L_{\mu\nu}\delta\tilde{g}^{\mu\nu} + \tilde{g}^{\mu\nu}\delta\mathcal{L}_{\mu\nu}}{\mathcal{L}^2} L - \frac{g_{\mu\nu}\delta g^{\mu\nu}}{2\mathcal{L}} L \right] \sqrt{-g} d^4\rho d^4\sigma \quad (5)$$

where the Lagrangian density is handled as a tensor.

By considering the cloud-world's boundary term: $\int_C g^{\mu\nu} \delta R_{\mu\nu} \sqrt{-g} d^4\sigma$, the variation in the Ricci curvature tensor $\delta R_{\mu\nu}$ can be expressed in terms of the covariant derivative of the difference between two Levi-Civita connections, the Palatini identity: $\delta R_{\mu\nu} = \nabla_\rho(\delta\Gamma_{\nu\mu}^\rho) - \nabla_\nu(\delta\Gamma_{\rho\mu}^\rho)$, where the variation with respect to the inverse metric $g^{\mu\nu}$ can be obtained by using the metric compatibility of the covariant derivative, $\nabla_\rho g^{\mu\nu} = 0$ [18], as $g^{\mu\nu} \delta R_{\mu\nu} = \nabla_\rho(g^{\mu\nu} \delta\Gamma_{\nu\mu}^\rho - g^{\mu\rho} \delta\Gamma_{\sigma\mu}^\sigma)$. Consequently, the boundary term as a total derivative for any tensor density is transformed based on Stokes' theorem with renaming the dummy indices as follows

$$\begin{aligned} \int_C [g^{\mu\nu} \delta R_{\mu\nu}] \sqrt{-g} d^4\rho &= \int_C [\nabla_\rho (g^{\mu\nu} \delta\Gamma_{\nu\mu}^\rho - g^{\mu\rho} \delta\Gamma_{\sigma\mu}^\sigma)] \sqrt{-g} d^4\rho \\ &= \int_C [\nabla_\mu A^\mu] \sqrt{-g} d^4\rho = \int_{\partial C} [K\epsilon] \sqrt{|q|} d^3\alpha \end{aligned} \quad (6)$$

The same is applied to bulk and Lagrangian boundary terms. Therefore, the transformed boundary action as well as the transformed global action in mixed component tensors are

$$\int_B \left[\frac{F_{\mu\lambda} F_\nu^\lambda \delta \tilde{g}^{\mu\nu}}{2\mu_0} - \frac{F_{\alpha\lambda} F^{\alpha\lambda} \tilde{g}_{\mu\nu} \delta \tilde{g}^{\mu\nu}}{8\mu_0} \right] \sqrt{-\tilde{g}} \left(\frac{\epsilon}{\mathcal{R}} \int_{\partial C} [K] \sqrt{|q|} d^3\alpha - \frac{R\epsilon}{\mathcal{R}^2} \int_{\partial C} [\mathcal{K}] \sqrt{|q|} d^3\alpha \right. \\ \left. - \frac{\epsilon}{\mathcal{L}} \int_{\partial C} [l] \sqrt{|q|} d^3\alpha - \frac{L\epsilon}{\mathcal{L}^2} \int_{\partial C} [\ell] \sqrt{|q|} d^3\alpha \right) d^4\sigma \quad (7)$$

where K and \mathcal{K} are the traces of the cloud-world and the bulk extrinsic curvatures, l and ℓ are the extrinsic traces of the Lagrangian density on the cloud-world and the bulk boundaries, q and q_b are the determinants of their induced metrics respectively, and ϵ equals 1 when the normal \hat{n}_u is a spacelike entity and equals -1 when it is a timelike entity. The boundary action should hold for any variation according to the principle of stationary action. Thus, the variation in the cloud-world boundary term is

$$\int_{\partial C} \left[K_{\mu\nu} \delta q^{\mu\nu} + q^{\mu\nu} \delta K_{\mu\nu} + K \frac{\delta \sqrt{|q|}}{\sqrt{|q|}} \right] \sqrt{|q|} d^3\alpha \quad (8)$$

where $K = K_{\mu\nu} q^{\mu\nu}$. By utilising Jacobi's formula for the determinant differentiation; thus, $\delta \sqrt{|q|} = -\sqrt{|q|} q_{\mu\nu} \delta q^{\mu\nu} / 2$ and by utilising the variation in the $q^{\mu\nu} q_{\mu\nu} = \delta_\nu^\mu$ as $q^{\mu\nu} = -q_{\mu\nu} \delta q^{\mu\nu} / \delta q_{\mu\nu}$; thus, the boundary term is

$$\int_{\partial C} \left[K_{\mu\nu} \delta q^{\mu\nu} - \frac{1}{2} K \left(q_{\mu\nu} \delta q^{\mu\nu} + 2 q_{\mu\nu} \frac{\delta K_{\mu\nu}}{\delta q_{\mu\nu} K} \delta q^{\mu\nu} \right) \right] \sqrt{|q|} d^3\alpha \quad (9)$$

here $\delta K_{\mu\nu} / \delta q_{\mu\nu} K = (\delta K_{\mu\nu} / K_{\mu\nu}) (q_{\mu\nu} / \delta q_{\mu\nu}) = \delta \ln K_{\mu\nu} / \delta \ln q_{\mu\nu}$ resembles the Ricci flow in a normalised form reflecting the conformal distortion in the boundary, which can be expressed as a positive function Ω^2 based on Weyl's conformal transformation [19] as $\tilde{q}_{\mu\nu} = q_{\mu\nu} \Omega^2$. So, Equation (9) is expressed as

$$\int_{\partial C} \left[K_{\mu\nu} \delta q^{\mu\nu} - \frac{1}{2} K \hat{q}_{\mu\nu} \delta q^{\mu\nu} \right] \sqrt{|q|} d^3\alpha \quad (10)$$

where $\hat{q}_{\mu\nu} = q_{\mu\nu} + 2\tilde{q}_{\mu\nu}$ denoting the conformally transformed induced metric tensor on

the cloud-world boundary. The same is applied for the bulk and Lagrangian boundary terms. Accordingly, the variation in the whole action is

$$\begin{aligned}
 \delta S = & \int_B \left[\frac{F_{\mu\lambda} F_\nu^\lambda}{2\mu_0} - \frac{F^{\alpha\lambda} F_{\alpha\lambda} \tilde{g}_{\mu\nu}}{8\mu_0} \right] \delta \tilde{g}^{\mu\nu} \sqrt{-\tilde{g}} \int_C \left[\frac{R_{\mu\nu}}{\mathcal{R}} - \frac{\mathcal{R}_{\mu\nu}}{\mathcal{R}^2} R - \frac{R g_{\mu\nu}}{2\mathcal{R}^2} \right] \delta g^{\mu\nu} \sqrt{-g} d^4 \rho d^4 \sigma + \\
 & \int_B \left[\left(\frac{F_{\mu\lambda} F_\nu^\lambda}{2\mu_0} - \frac{F^{\alpha\lambda} F_{\alpha\lambda} \tilde{g}_{\mu\nu}}{8\mu_0} \right) \frac{1}{\mathcal{L}} \right] \delta \tilde{g}^{\mu\nu} \sqrt{-\tilde{g}} \int_C \left[L_{\mu\nu} - \frac{\mathcal{L}_{\mu\nu}}{\mathcal{L}} L - \frac{L g_{\mu\nu}}{2\mathcal{L}} \right] \delta g^{\mu\nu} \sqrt{-g} d^4 \rho d^4 \sigma + \\
 & \int_B \left[\left(\frac{F_{\mu\lambda} F_\nu^\lambda}{2\mu_0} - \frac{F^{\alpha\lambda} F_{\alpha\lambda} \tilde{g}_{\mu\nu}}{8\mu_0} \right) \frac{\epsilon}{\mathcal{R}} \right] \delta \tilde{g}^{\mu\nu} \sqrt{-\tilde{g}} \int_{\partial C} \left[K_{\mu\nu} - \frac{K \hat{q}_{\mu\nu}}{2} \right] \delta q^{\mu\nu} \sqrt{|q|} d^3 \alpha d^4 \sigma - \\
 & \int_B \left[\left(\frac{F_{\mu\lambda} F_\nu^\lambda}{2\mu_0} - \frac{F^{\alpha\lambda} F_{\alpha\lambda} \tilde{g}_{\mu\nu}}{8\mu_0} \right) \frac{R\epsilon}{\mathcal{R}^2} \right] \delta \tilde{g}^{\mu\nu} \sqrt{-\tilde{g}} \int_{\partial C} \left[\mathcal{K}_{\mu\nu} - \frac{\mathcal{K} \hat{q}_{\mu\nu}}{2} \right] \delta q^{\mu\nu} \sqrt{|q|} d^3 \alpha d^4 \sigma + \\
 & \int_B \left[\left(\frac{F_{\mu\lambda} F_\nu^\lambda}{2\mu_0} - \frac{F^{\alpha\lambda} F_{\alpha\lambda} \tilde{g}_{\mu\nu}}{8\mu_0} \right) \frac{\epsilon}{\mathcal{L}} \right] \delta \tilde{g}^{\mu\nu} \sqrt{-\tilde{g}} \int_{\partial C} \left[l_{\mu\nu} - \frac{l \hat{q}_{\mu\nu}}{2} \right] \delta q^{\mu\nu} \sqrt{|q|} d^3 \alpha d^4 \sigma - \\
 & \int_B \left[\left(\frac{F_{\mu\lambda} F_\nu^\lambda}{2\mu_0} - \frac{F^{\alpha\lambda} F_{\alpha\lambda} \tilde{g}_{\mu\nu}}{8\mu_0} \right) \frac{L\epsilon}{\mathcal{L}^2} \right] \delta \tilde{g}^{\mu\nu} \sqrt{-\tilde{g}} \int_{\partial C} \left[\ell_{\mu\nu} - \frac{\ell \hat{q}_{\mu\nu}}{2} \right] \delta q^{\mu\nu} \sqrt{|q|} d^3 \alpha d^4 \sigma
 \end{aligned} \quad (11)$$

By encapsulating the new Lagrangian terms on the boundaries into an extended stress-energy tensor that can be defined as $\bar{T}_{\mu\nu} := (L_{\mu\nu} - L \hat{g}_{\mu\nu}/2) - (l_{\mu\nu} - l \hat{q}_{\mu\nu}/2)$ which counts for both the flux and energy density of the cloud-world and the electromagnetic energy flux from its boundary over conformal time where $\hat{g}_{\mu\nu} = g_{\mu\nu} + 2\tilde{g}_{\mu\nu}$ is the conformally transformed metric of $\tilde{g}_{\mu\nu} = \mathcal{L}_{\mu\nu}/\mathcal{L} = \mathcal{L}_{\mu\nu}/\mathcal{L}_{\mu\nu} \tilde{g}^{\mu\nu}$. No energy flux from bulk's boundary. Additionally, the outcomes of the global part of the action resembled the electromagnetic stress-energy tensor as $\mathcal{T}_{\mu\nu} := (F_{\mu\lambda} F_\nu^\lambda - F^{\alpha\lambda} F_{\alpha\lambda} \tilde{g}_{\mu\nu}/4)/\mu_0$ representing the energy density present in the bulk as the vacuum energy density. Further, from Equations (1) and (11), $\mathcal{T}_{\mu\nu} := E_D = \mathcal{L} = \mathcal{R}c^4/8\pi G_t$, which is proportional to the fourth power of the speed of light that in turn is proportional to the frequency, which can be in accordance with the frequency cut-off predictions of the vacuum energy density in the quantum field theory [20,21]. By choosing ϵ as a timelike entity and applying the principle of stationary action yields

$$\frac{R_{\mu\nu}}{\mathcal{R}} - \frac{1}{2} \frac{R}{\mathcal{R}} g_{\mu\nu} - \frac{\mathcal{R}_{\mu\nu}}{\mathcal{R}^2} R + \frac{R \left(\mathcal{K}_{\mu\nu} - \frac{1}{2} \mathcal{K} \hat{q}_{\mu\nu} \right) - \mathcal{R} \left(K_{\mu\nu} - \frac{1}{2} K \hat{q}_{\mu\nu} \right)}{\mathcal{R}^2} = \frac{\bar{T}_{\mu\nu}}{\mathcal{T}_{\mu\nu}} \quad (12)$$

The extended field equations can be interpreted as indicating that the induced curvature over the bulk (pre-existing) curvature equals the ratio of the imposed energy density and its flux to the vacuum energy density and its flux throughout the expanding/contracting Universe. By utilizing Equations (1) and (11) that state $\mathcal{T}_{\mu\nu} = E_D = \mathcal{R}c^4/8\pi G_t$, the field equations can be simplified to

$$R_{\mu\nu} - \frac{1}{2} R \hat{g}_{\mu\nu} + \frac{R \left(\mathcal{K}_{\mu\nu} - \frac{1}{2} \mathcal{K} \hat{q}_{\mu\nu} \right) - \mathcal{R} \left(K_{\mu\nu} - \frac{1}{2} K \hat{q}_{\mu\nu} \right)}{\mathcal{R}} = \frac{8\pi G_t}{c^4} \bar{T}_{\mu\nu} \quad (13)$$

where $\hat{g}_{\mu\nu} = g_{\mu\nu} + 2\tilde{g}_{\mu\nu}$ and $\tilde{g}_{\mu\nu} = \mathcal{R}_{\mu\nu}/\mathcal{R} = \mathcal{R}_{\mu\nu}/\mathcal{R}_{\mu\nu} \tilde{g}^{\mu\nu}$. $\hat{g}_{\mu\nu}$ denotes the conformally transformed metric accounting for both the cloud-world and the bulk metrics whereas Einstein spaces are a subclass of the conformal space [16]. The evolution in G_t can accommodate the bulk curvature evolution over the conformal time against constant G for a special flat spacetime case. The new boundary term is only significant at high-energy limits such as within black holes [29]. The field equations could remove the singularities and satisfy a conformal invariance theory.

3. Galaxy Formation, Evolution and Rotation

The entire contribution comes from the boundary term when calculating the black hole entropy using the semiclassical approach [29,31]. Applying this concept and by rearranging the field equations for this setting as

$$\frac{R_{\mu\nu}}{\mathcal{R}} - \frac{1}{2} \frac{R}{\mathcal{R}} g_{\mu\nu} - \frac{\mathcal{R}_{\mu\nu}}{\mathcal{R}^2} R = \frac{\bar{T}_{\mu\nu}}{\mathcal{T}_{\mu\nu}} - \frac{R \left(\mathcal{K}_{\mu\nu} - \frac{1}{2} \mathcal{K} \hat{q}_{\mu\nu} \right) - \mathcal{R} \left(K_{\mu\nu} - \frac{1}{2} K \hat{q}_{\mu\nu} \right)}{\mathcal{R}^2} = 0 \quad (13)$$

The extended field equations can describe the interaction between a 4D relativistic cloud-world of intrinsic $R_{\mu\nu}$ and extrinsic $K_{\mu\nu}$ curvatures with stress-energy $\bar{T}_{\mu\nu}$ and the 4D global bulk of intrinsic $\mathcal{R}_{\mu\nu}$ and extrinsic $\mathcal{K}_{\mu\nu}$ curvatures with stress-energy $\mathcal{T}_{\mu\nu}$. From Equation (13), the field equations yield

$$R_{\mu\nu} = \frac{1}{2} R g_{\mu\nu} + \frac{\mathcal{R}_{\mu\nu}}{\mathcal{R}} R = \frac{1}{2} R (g_{\mu\nu} + 2\tilde{g}_{\mu\nu}) = \frac{1}{2} R \hat{g}_{\mu\nu} = \frac{1}{2} R g_{\mu\nu} (1 + 2\Omega^2) = 0 \quad (14)$$

where $\tilde{g}_{\mu\nu} = \mathcal{R}_{\mu\nu}/\mathcal{R} = \mathcal{R}_{\mu\nu}/\mathcal{R}_{\mu\nu} \tilde{g}^{\mu\nu}$ is the conformal bulk metric, which can be expressed as proportional to cloud-world metric $q_{\mu\nu}$ as $\tilde{g}_{\mu\nu} = q_{\mu\nu} \Omega^2$ utilizing Ω^2 , the conformal function.

The conformally transformed metric $\hat{g}_{\mu\nu} = g_{\mu\nu} (1 + 2\Omega^2)$ can be expressed as

$$ds^2 = -A(r)(1 + 2\Omega^2(r))c^2 dt^2 + S(B(r)(1 + 2\Omega^2(r)))dr^2 + r^2 d\theta^2 + r^2 \sin^2 \theta d\phi^2 \quad (15)$$

where A, B and Ω^2 are functions of the radius r and S is a dimensionless conformal scale factor. By performing coordinate transformation as follows

$$ds^2 = -(A(\lambda) + 2A(\lambda)\Omega^2(\lambda))c^2 dt^2 + ((B(\lambda) + 2B(\lambda)\Omega^2(\lambda))d\lambda^2 + \lambda^2 d\theta^2 + \lambda^2 \sin^2 \theta d\phi^2) \quad (16)$$

The Christoffel symbols of this metric are

$$\begin{aligned} \Gamma_{00}^1 &= \frac{\dot{A}(1 + 2\Omega^2) + 4A\dot{\Omega}}{2(B + 2B\Omega^2)}, & \Gamma_{01}^0 &= \frac{\dot{A}(1 + 2\Omega^2) + 4A\dot{\Omega}}{2(A + 2A\Omega^2)}, & \Gamma_{11}^1 &= \frac{\dot{B}(1 + 2\Omega^2) + 4B\dot{\Omega}}{2(B + 2B\Omega^2)} \\ \Gamma_{22}^1 &= \frac{-\lambda}{(B + 2B\Omega^2)}, & \Gamma_{33}^1 &= \frac{\lambda \sin^2 \theta}{(B + 2B\Omega^2)}, & \Gamma_{21}^2 &= \Gamma_{31}^3 = \frac{1}{\lambda} \\ \Gamma_{33}^2 &= -\sin \theta \cos \theta, & \Gamma_{32}^3 &= \frac{\cos \theta}{\sin \theta} \end{aligned} \quad (17)$$

The Ricci tensor components are

$$\begin{aligned} R_{00} &= -\frac{1}{2} \left(\frac{\ddot{A}(1 + 2\Omega^2 + 4\dot{\Omega}) + 4A\ddot{\Omega} + 4\dot{\Omega}\dot{A}}{B + 2B\Omega^2} - \frac{\dot{A}(1 + 2\Omega^2) + 4A\dot{\Omega}}{(B + 2B\Omega^2)^2} \right) \\ &\quad - \frac{1}{4} \frac{\dot{A}(1 + 2\Omega^2) + 4A\dot{\Omega}}{(B + 2B\Omega^2)^2} + \frac{(\dot{A}(1 + 2\Omega^2) + 4A\dot{\Omega})^2}{4(A + 2A\Omega^2)(B + 2B\Omega^2)} - \frac{1}{\lambda} \frac{\dot{A}(1 + 2\Omega^2) + 4A\dot{\Omega}}{(B + 2B\Omega^2)} \end{aligned} \quad (18)$$

$$R_{11} = -\frac{1}{2} \left(\frac{\ddot{A}(1+2\Omega^2+4\dot{\Omega})+4A\ddot{\Omega}+4\dot{\Omega}\dot{A}}{(A+2A\Omega^2)} - \frac{\dot{A}(1+2\Omega^2)+4A\dot{\Omega}}{(A+2A\Omega^2)^2} \right) \quad (19)$$

$$+\frac{1}{4} \frac{\dot{A}(1+2\Omega^2)+4A\dot{\Omega}}{(A+2A\Omega^2)^2} + \frac{(\dot{A}(1+2\Omega^2)+4A\dot{\Omega})^2}{4(A+2A\Omega^2)(B+2B\Omega^2)} - \frac{1}{\lambda} \frac{\dot{B}(1+2\Omega^2)+4B\dot{\Omega}}{B+2B\Omega^2}$$

$$R_{22} = \frac{1}{(B+2B\Omega^2)} - \frac{\lambda}{2(B+2B\Omega^2)} \left(\frac{\dot{B}(1+2\Omega^2)+4B\dot{\Omega}}{(B+2B\Omega^2)} - \frac{\dot{A}(1+2\Omega^2)+4A\dot{\Omega}}{(A+2A\Omega^2)} \right) - 1 \quad (20)$$

$$R_{33} = \frac{1}{(B+2B\Omega^2)} - \frac{\lambda}{2(B+2B\Omega^2)} \left(\frac{\dot{B}(1+2\Omega^2)+4B\dot{\Omega}}{(B+2B\Omega^2)} - \frac{\dot{A}(1+2\Omega^2)+4A\dot{\Omega}}{(A+2A\Omega^2)} \right) \sin^2\theta - 1 \quad (21)$$

Using Ricci tensor components gives

$$(\dot{A}(1+2\Omega^2)+4A\dot{\Omega})(B+2B\Omega^2) + (A+2A\Omega^2)(\dot{B}(1+2\Omega^2)+4B\dot{\Omega}) = 0 \quad (22)$$

Equation (22) leads to

$$B+2B\Omega^2 = \frac{c}{A+2A\Omega^2} \quad (23)$$

where c is a constant. The metric should approach the Minkowski metric at $\lambda \rightarrow \infty$; thus:

$$\lim_{\lambda \rightarrow \infty} (A(\lambda) + 2A(\lambda)\Omega^2(\lambda)) = 1, \quad (24)$$

Applying the weak-field limit:

$$-A(\lambda)(1+2\Omega^2(\lambda)) = -\left(1 + \frac{2\varphi}{c^2}\right) \quad (25)$$

where $\varphi = -GM/\lambda$. Combining Equations (23-25) yields

$$\Omega^2(\lambda) = -\frac{GM}{\lambda c^2}, \quad A(\lambda) = 1, \quad B(\lambda) = \left(1 - 2\frac{GM}{\lambda c^2}\right)^{-2} \quad (26)$$

Equation 26 shows the conformal function $\Omega^2(\lambda)$ has a minus sign, revealing a spatial shrinking through evolving in the conformal time. This agrees with the vortex model which can occur due to the high-speed spinning. By performing coordinate retransformation to $\Omega^2(r)$ and S and submitting Equations (26) to Equation (15) give

$$ds = -\left(1 - 2\frac{GM}{rc^2}\right)c^2dt^2 + S\left(\frac{dr^2}{1 - 2\frac{GM}{rc^2}} + r^2d\theta^2 + r^2\sin^2\theta d\phi^2\right) \quad (27)$$

where S is the dimensionless spatial scale factor to account for the conformal shrinking. Equation (27) has resembled the Schwarzschild metric which verifies the derivations with an interpolation of the A, B, S and Ω^2 functions. The scale factor S of the cloud-world as a function of the conformal time can be visualized by using Flamm's paraboloid as shown in Figure 1.

Figure 1 shows the evolution of the 4D cloud-world through its travel and spin in the conformal space-time of the 4D bulk.

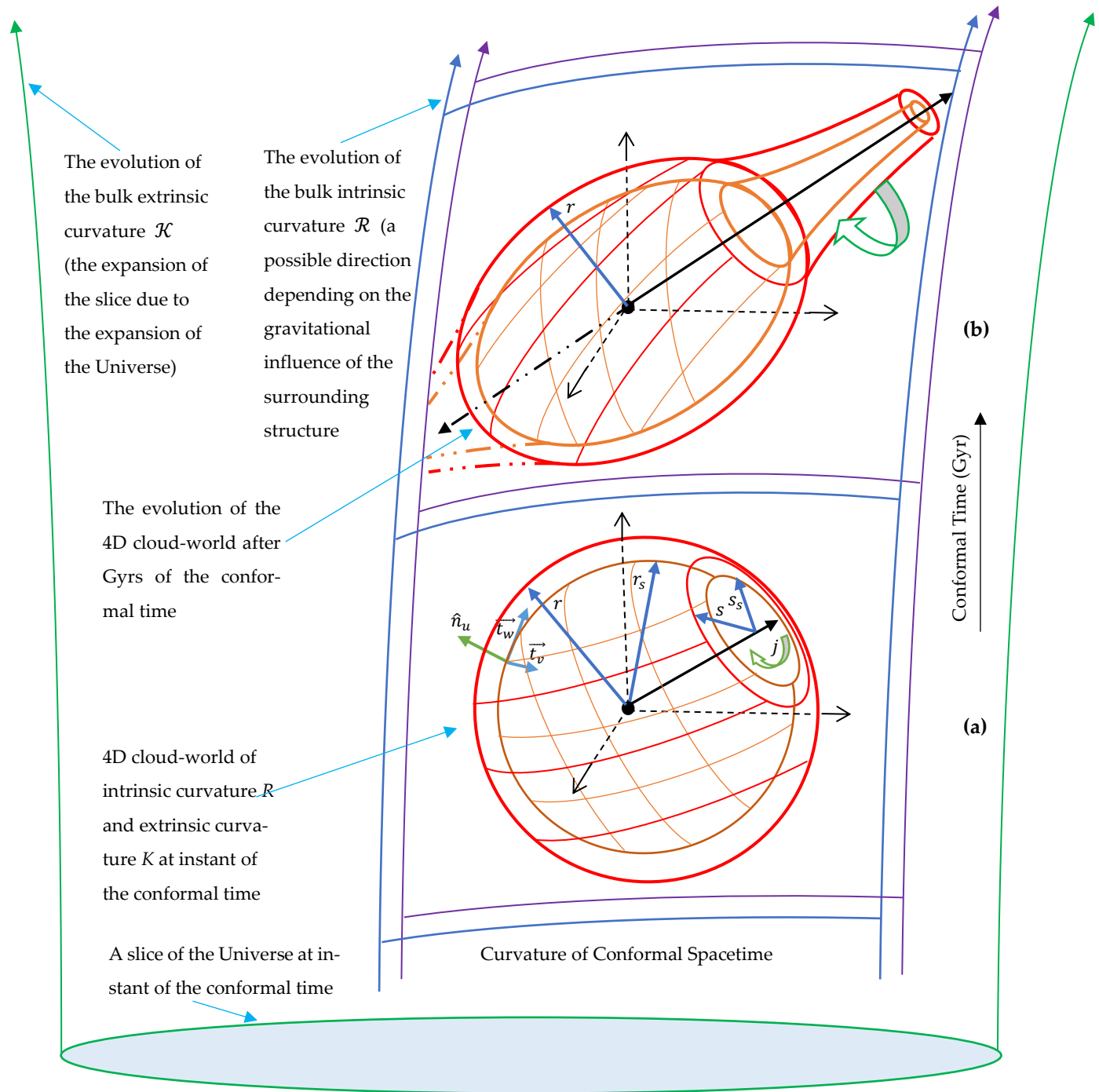


Figure 1. The hypersphere of a compact core of a galaxy (the red-orange 4D cloud-world) along with its travel and spin through the conformal spacetime (the blue-purple 4D bulk representing the background of distinctive curvature evolving over the conformal time).

Orbiting a vortex could explain the observations of the G2 cloud which only faced drag forces and was not destroyed, [11,12], Further, the observation of the superluminal motion in the x-ray jet of M87 [33] could be travel through these traversable wormholes.

To evaluate the influence of the spinning momentum and the curvature of the background on the core of the galaxy and the surrounding gas clouds (the spiral arms), a fluid simulation was performed based on Newtonian dynamics by using the Fluid Pressure and Flow software [34]. In this simulation, the fluid was deemed to represent the spacetime continuum throughout incrementally flattening curvature paths representing conformal curvature evolution to analyze the external momenta exerted on objects flowing throughout the incrementally flattening curvatures. The momenta yielded by the fluid simulation were used to simulate a spiral galaxy as a forced vortex as shown in Figure 2.

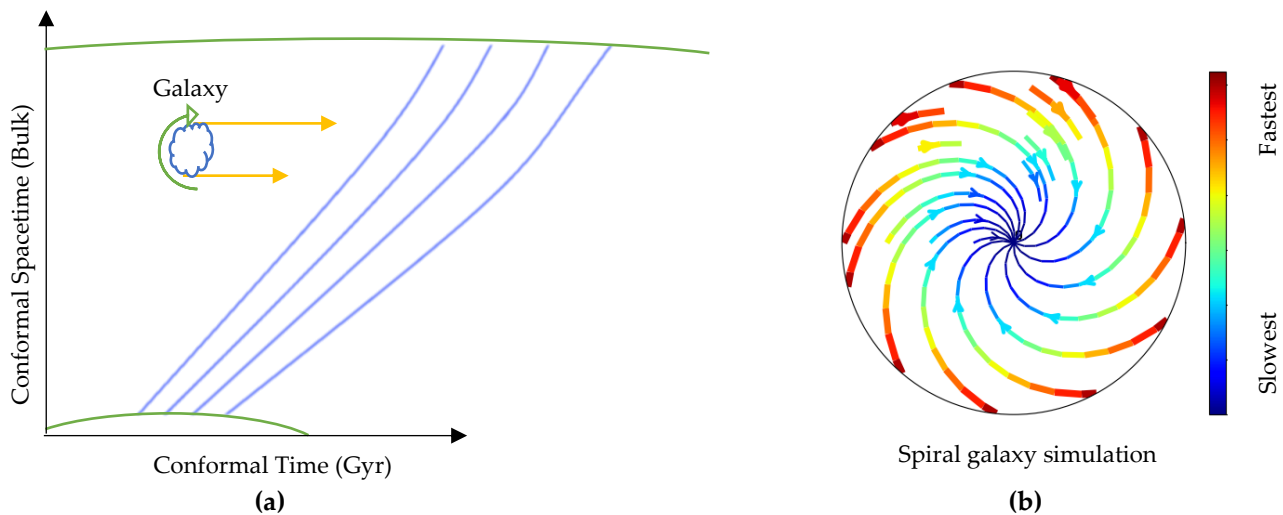


Figure 2. (a) External fields exerted on a galaxy due to the spacetime conformal curvature evolution. Green curves represent the curvature of spacetime worldlines. Blue curves represent the simulated spacetime continuum. (b) Simulation of spiral galaxy rotation. Blue represents the slowest tangential speeds and red represents the fastest speeds.

The simulation shows that the tangential speeds of the outer parts of the spiral galaxy are rotating faster in comparison with the rotational speeds of the inner parts, which resembles observations of galaxy rotation except the simulation used ideal fluid.

4. Conclusions and Future Works

In this study, extended field equations are presented where a galaxy formation scenario is derived in which the bulk is regarded as background or the 4D conformal bulk of distinct curvature that can evolve over the conformal time, where the recent PL18 release has preferred a positively curved early Universe with a confidence level higher than 99%. Throughout this bulk, branes or 4D relativistic cloud-worlds flow and spin.

The findings of galaxy formation showed that the core of the galaxy forms as a central vortex with an event horizon leading to opposite traversable wormholes that shrink through evolving in the conformal time. It revealed that the galaxy and its core form at the same process, while the gas clouds outside the core form the spiral arms owing to the fast-rotating core that induces the frame-dragging. Orbiting a wormhole and far away from the central event horizon can explain the observation of the G2 cloud which only faced the drag effects. The observation of the superluminal motion in the x-ray jet of M87 could be travelling through these traversable wormholes. The formation of the galaxy and its core at the same process could elucidate the formation of supermassive compact galaxy cores with a mass of $\sim 10^9 M_{\odot}$ at just 6% of the current Universe age and might solve the black hole hierarchy problem. The derived field equations should be applied to atoms and electron clouds as well that with galaxies, which can be investigated in future works.

Conflicts of Interest: The author declares no conflict of interest.

References

- [1] Kassin S A, Weiner B J, Faber S M, Gardner J P, Willmer C N A, Coil A L, Cooper M C, Devriendt J, Dutton A A, Guhathakurta P, Koo D C, Metevier A J, Noeske K G and Primack J R 2012 THE EPOCH OF DISK SETTLING: $z \sim 1$ TO NOW *Astrophys. J.* **758** 106
- [2] Kassin S A, Brooks A, Governato F, Weiner B J and Gardner J P 2014 *KINEMATIC EVOLUTION OF SIMULATED STAR-FORMING GALAXIES*
- [3] Chae K H, Lelli F, Desmond H, McGaugh S S, Li P and Schombert J M 2020 Testing the strong equivalence principle: Detection of the external field effect in rotationally supported galaxies *arXiv* **904** 51
- [4] Kroupa P 2012 The dark matter crisis: Falsification of the current standard model of cosmology *Publ. Astron. Soc. Aust.* **29** 395–433
- [5] McGaugh S S 2012 The baryonic tully-fisher relation of gas-rich galaxies as a test of Λ CDM and MOND *Astron. J.* **143** 40
- [6] Amon A, Gruen D, Troxel M A, MacCrann N, Dodelson S, Choi A, Doux C, Secco L F, Samuroff S, Krause E, Cordero J, Myles J, DeRose J, Wechsler R H, Gatti M, Navarro-Alsina A, Bernstein G M, Jain B, Blazek J, Alarcon A, Ferté A, Raveri M, Lemos P, Campos A, Prat J, Sánchez C, et al 2021 Dark Energy Survey Year 3 Results: Cosmology from Cosmic Shear and Robustness to Data Calibration **21** 68
- [7] DES Collaboration, Abbott T M C, Aguena M, Alarcon A, Allam S, Alves O, Amon A, Andrade-Oliveira F, Annis J, Avila S, Bacon D, Baxter E, Bechtol K, Becker M R, Bernstein G M, Bhargava S, Birrer S, Blazek J, Brandao-Souza A, Bridle S L, Brooks D, Buckley-Geer E, Burke D L, Camacho H, Campos A, Rosell A C, Kind M C, Carretero J, Castander F J, Cawthon R, Chang C, Chen A, Chen R, Choi A, Conselice C, Cordero J, Costanzi M, Croce M, da Costa L N, Pereira M E da S, Davis C, Davis T M, De Vicente J, DeRose J, Desai S, Di Valentino E, Diehl H T, Dietrich J P, Dodelson S, Doel P, Doux C, Drlica-Wagner A, Eckert K, Eifler T F, Elsner F, Elvin-Poole J, Everett S, Evrard A E, Fang X, Farahi A, Fernandez E, Ferrero I, Ferté A, Fosalba P, Friedrich O, Frieman J, García-Bellido J, Gatti M, Gaztanaga E, Gerdes D W, Giannantonio T, Giannini G, Gruen D, Gruendl R A, Gschwend J, Gutierrez G, Harrison I, Hartley W G, Herner K, Hinton S R, Hollowood D L, Honscheid K, Hoyle B, Huff E M, Huterer D, Jain B, James D J, Jarvis M, Jeffrey N, Jeltema T, Kovacs A, Krause E, Kron R, Kuehn K, Kuropatkin N, Lahav O, Leget P-F, Lemos P, et al 2021 Dark Energy Survey Year 3 Results: Cosmological Constraints from Galaxy Clustering and Weak Lensing **54** 30
- [8] Guo Q, Hu H, Zheng Z, Liao S, Du W, Mao S, Jiang L, Wang J, Peng Y, Gao L, Wang J and Wu H 2019 Further evidence for a population of dark-matter-deficient dwarf galaxies *Nat. Astron.* **4** 246–51
- [9] van Dokkum P, Danieli S, Abraham R, Conroy C and Romanowsky A J 2019 A Second Galaxy Missing Dark Matter in the NGC 1052 Group *Astrophys. J.* **874** L5
- [10] Danieli S, van Dokkum P, Conroy C, Abraham R and Romanowsky A J 2019 Still Missing Dark Matter: KCWI High-resolution Stellar Kinematics of NGC1052-DF2 *Astrophys. J.* **874** L12
- [11] Burkert A, Scharntmann M, Alig C, Gillessen S, Genzel R, Fritz T K and Eisenhauer F 2012 Physics of the galactic center cloud G2, on its way toward the supermassive black hole *Astrophys. J.* **750** 58
- [12] Becerra-Vergara E A, Argüelles C R, Krut A, Rueda J A and Ruffini R 2021 Hinting a dark matter nature of Sgr A* via the S-stars *Mon. Not. R. Astron. Soc. Lett.* **505** L64–8
- [13] Di Valentino E, Melchiorri A and Silk J 2020 Planck evidence for a closed Universe and a possible crisis for cosmology *Nat. Astron.* **4** 196–203
- [14] Handley W 2021 Curvature tension: Evidence for a closed universe *Phys. Rev. D* **103** L041301
- [15] Landau L D 1986 *Theory of Elasticity* (Elsevier)
- [16] Kozameh C, Newman E, gravitation K T-G relativity and and 1985 undefined 1985 Conformal Einstein spaces *Springer*
- [17] Camarena D and Marra V 2020 Local determination of the Hubble constant and the deceleration parameter *Phys. Rev. Res.*

2 013028

- [18] S. M. Carroll 2003 Spacetime and Geometry: An Introduction to General Relativity
- [19] Straub W O 2006 *Simple Derivation of the Weyl Conformal Tensor*
- [20] Rugh S E and Zinkernagel H 2000 The Quantum Vacuum and the Cosmological Constant Problem *Stud. Hist. Philos. Sci. Part B - Stud. Hist. Philos. Mod. Phys.* **33** 663–705
- [21] Gómez-Valent A 2017 *VACUUM ENERGY IN QUANTUM FIELD THEORY AND COSMOLOGY*
- [22] Gannouji R, Kazantzidis L, Perivolaropoulos L and Polarski D 2018 *Consistency of Modified Gravity with a decreasing $G_{\text{eff}}(z)$ in a Λ CDM background*
- [23] Saridakis E N, Lazkoz R, Salzano V, Moniz P V, Capozziello S, Jiménez J B, De Laurentis M, Olmo G J, Akrami Y, Bahamonde S, Blázquez-Salcedo J L, Böhmer C G, Bonvin C, Bouhmadi-López M, Brax P, Calcagni G, Casadio R, Cembranos J A R, de la Cruz-Dombriz Á, Davis A-C, Delhom A, Di Valentino E, Dialektopoulos K F, Elder B, Ezquiaga J M, Frusciante N, Garattini R, Gergely L Á, Giusti A, Heisenberg L, Hohmann M, Iosifidis D, Kazantzidis L, Kleihaus B, Koivisto T S, Kunz J, Lobo F S N, Martinelli M, Martín-Moruno P, Mimoso J P, Mota D F, Peirone S, Perivolaropoulos L, Pettorino V, Pfeifer C, Pizzuti L, Rubiera-Garcia D, Said J L, Sakellariadou M, Saltas I D, Mancini A S, Voicu N and Wojnar A 2021 Modified Gravity and Cosmology: An Update by the CANTATA Network *Konstantinos F. Dialektopoulos* **12** 25
- [24] Sobral D, Smail I, Best P N, Geach J E, Matsuda Y, Stott J P, Cirasuolo M and Kurk J 2012 *A large H α survey at $z = 2.23, 1.47, 0.84$ & 0.40 : the 11 Gyr evolution of star-forming galaxies from HiZELS* vol 000
- [25] Quinn T, Parks H, Speake C and Davis R 2013 Improved determination of G using two methods *Phys. Rev. Lett.* **111** 101102
- [26] Wilczynska M R, Webb J K, Bainbridge M, Barrow J D, Bosman S E I, Carswell R F, Dąbrowski M P, Dumont V, Lee C C, Leite A C, Leszczyńska K, Liske J, Marosek K, Martins C J A P, Milaković D, Molaro P and Pasquini L 2020 Four direct measurements of the fine-structure constant 13 billion years ago *Sci. Adv.* **6** eaay9672
- [27] Donoghue J F 2003 Spatial and temporal gradients in the cosmological constant *J. High Energy Phys.* **7** 1115–29
- [28] Uzan J P 2011 Varying constants, gravitation and cosmology *Living Rev. Relativ.* **14** 1–155
- [29] Dyer E and Hinterbichler K 2009 Boundary terms, variational principles, and higher derivative modified gravity *Phys. Rev. D - Part. Fields, Gravit. Cosmol.* **79**
- [30] Penrose R 2005 *The Road to Reality: A Complete Guide to the Laws of the Universe*
- [31] Brown J D and York J W 1993 Microcanonical functional integral for the gravitational field *Phys. Rev. D* **47** 1420–31
- [32] Pavel Grinfeld 2013 *Introduction to Tensor Analysis and the Calculus of Moving Surfaces* (Springer)
- [33] Snios B, Nulsen P E J, Kraft R P, Cheung C C, Meyer E T, Forman W R, Jones C and Murray S S 2019 *Detection of Superluminal Motion in the X-Ray Jet of M87*
- [34] Reid S, Podolefsky H and Pual A 2013 Fluid Pressure and Flow, PhET Interactive Simulations.